



ELSEVIER

International Journal of Refrigeration 26 (2003) 232–239

REVUE INTERNATIONALE DU FROID
INTERNATIONAL JOURNAL OF
refrigeration

www.elsevier.com/locate/ijrefrig

Detailed simulation of fluted tube water heating condensers

P.G. Rousseau, M. van Eldik*, G.P. Greyvenstein

*School of Mechanical and Materials Engineering, Potchefstroom University for CHE, Private Bag X6001,
Potchefstroom 2520, South Africa*

Received 24 October 2001; received in revised form 11 June 2002; accepted 28 June 2002

Abstract

Fluted tube-in-tube condensers are key components in advanced energy efficient water heating heat pumps. Therefore, there exists a need for a computer design tool that incorporates all the essential features of these heat exchangers. This paper describes the development of a detailed model to simulate fluted tube refrigerant-to-water condensers. The model allows the surface area to be divided into any number of sections for which all the refrigerant and water properties can be evaluated. This allows for the extension of the model to simulate heat exchangers for cycles employing zeotropic refrigerant mixtures. For the waterside existing empirical equations are used for both friction and heat transfer. However, on the refrigerant side no correlations are available in the literature to calculate friction and heat transfer coefficients. The approach followed in this paper is therefore to use existing smooth tube correlations combined with enhancement ratios based on correlations available for helical coils as well as enhancement factors based on empirical data for fluted tube condensers. The model is validated with the aid of results from independent tests on two commercial fluted tube heat exchangers. The average difference between the simulated and measured pressure drops is 7.27% and the average difference for the log mean temperature difference (LMTD) is 4.41%.

© 2003 Elsevier Science Ltd and IIR. All rights reserved.

Keywords: Heat pump; Condenser; Tube; Enhanced surface; Water; Heating; Performance; Modelling

Modélisation des performances de condenseurs de pompe à chaleur à tubes rainurés, pour chauffage d'eau

Mots clés : Pompe à chaleur ; Condenseur ; Tube ; Surface augmentée ; Eau ; Chauffage ; Performance ; Modélisation

1. Introduction

The refrigerant-to-water heat exchanger for condensing the refrigerant forms an important component of any heat pump/refrigeration cycle. One reason for this is that the overall effectiveness of the cycle is influenced by the effectiveness of heat exchange in the condenser. It is desirable to keep the temperature difference, ΔT ,

between the refrigerant and the water in the condenser as small as possible. This leads to a lowering in the ΔT over which heat must be transferred and thus to an increase in the coefficient of performance (COP). The type of water heat exchanger concentrated on in this study is a fluted tube heat exchanger, with water in the centre in counter-flow with the refrigerant in the twisted annulus. Fig. 1 illustrates the geometry of a typical fluted tube heat exchanger.

Fluted tube condensers are able to produce high heat transfer coefficients on both sides of the transfer surface by enhancing the flow conditions for both sides. The

* Corresponding author. Tel.: +27-18-299-1324; fax: +27-18-299-1320.

E-mail addresses: mgimve@puknet.puk.ac.za.

Nomenclature			
θ	Helix angle	h_r	Refrigerant enthalpy (J kg^{-1})
θ^*	Non-dimensional helix angle	h_{tp}	Two-phase heat transfer coefficient ($\text{W m}^{-2} \text{K}^{-1}$)
μ	Viscosity ($\text{N}\cdot\text{s m}^{-2}$)	k	Thermal conductivity ($\text{W m}^{-1} \text{K}^{-1}$)
η	Effectiveness	L	Length of fluted tube (m)
ρ	Density (kg m^{-3})	\dot{m}	Mass flow rate (kg s^{-1})
A_{sc}	Sub-cooled area (m^2)	N	Number of flute starts
A_{sh}	Superheated area (m^2)	NTU	Number of transfer units
A_{tp}	Two-phase area (m^2)	Nu	Nusselt number
A_{total}	Total heat transfer area (m^2)	$\text{Nu}_{helical}$	Nusselt number for helical coils
c_p	Specific heat capacity ($\text{J kg}^{-1} \text{K}^{-1}$)	$\text{Nu}_{straight}$	Nusselt number for straight tubes
$\Delta p_{helical}$	Pressure drop in helical coils (Pa)	p	Flute pitch (m)
$\Delta p_{straight}$	Pressure drop in straight tubes (Pa)	p^*	Non-dimensional flute pitch
d_{coil}	Helical friction parameter (m)	pr	Pressure ratio
D_{ho}	Hydraulic outside diameter (m)	Pr	Prandtl number
D_{vi}	Volume based inside diameter (m)	Q	Heat transfer (W)
D_{vo}	Volume based outside diameter (m)	Q_{max}	Maximum heat transfer (W)
e	Flute depth (m)	r_f	Friction enhancement ratio
e^*	Non-dimensional flute depth	r_h	Heat transfer enhancement ratio
e_r	Friction enhancement factor	Re_w	Reynolds number water
e_h	Heat transfer enhancement factor	Re_r	Reynolds number refrigerant
f	Friction factor	Re_v	Vapour Reynolds number
$f_{helical}$	Helical coil friction factor	t	Wall thickness (m)
$f_{straight}$	Straight tube friction factor	T_r	Refrigerant temperature (K)
h_i	Inside heat transfer coefficient ($\text{W m}^{-2} \text{K}^{-1}$)	T_w	Water temperature (K)
h_{liq}	Liquid heat transfer coefficient ($\text{W m}^{-2} \text{K}^{-1}$)	U	Overall heat transfer coefficient ($\text{W m}^{-2} \text{K}^{-1}$)
		Vol	Volume enclosed inside fluted tube (m^3)
		x	Quality

water heat transfer coefficient is improved by micro-circulation of the water without a significant increase in the pressure drop. Heat transfer in the annulus is improved by the following two phenomena. In the first instance the condensate is drawn towards the corners of the channels by surface tension, clearing the remaining surface in contact with the hot gas. Secondly, the liquid phase experiences some micro-circulation, particularly towards the outlet side, leading to the replacement of cold liquid next to the surface with hotter liquid. This

leads to only a relatively small increase in the pressure drop.

In the condenser a counter-flow arrangement is used to obtain the maximum heat transfer where it is possible to achieve outlet water temperatures above the condensing temperature and approaching the superheat temperature of the refrigerant gas. This is illustrated in Fig. 2 where the cold inlet water is at T_{w1} and the hot outlet water is at T_{w4} . It is clear that T_{w4} is higher than the refrigerant condensing temperature, which is

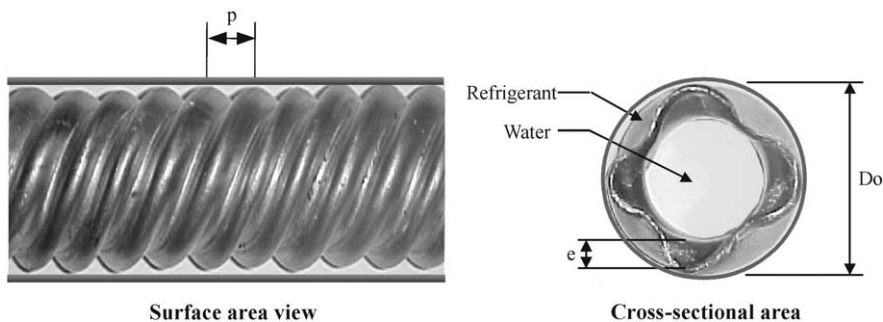


Fig. 1. Geometry of fluted tube condenser.

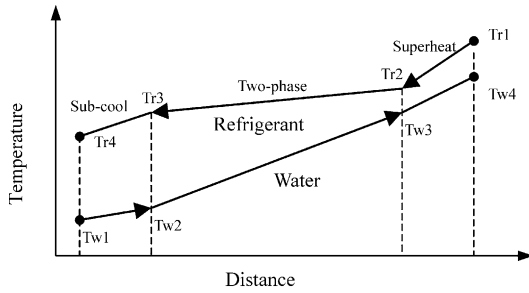


Fig. 2. Temperature distribution in condenser.

between T_{r2} and T_{r3} due to the water exchanging heat with superheated refrigerant gas which is at a higher temperature than the condensing temperature. The reason for the refrigerant being sub-cooled (T_{r4}), is that this leads to a lower enthalpy and quality at the entrance to the evaporator. This means that more heat transfer can take place in the evaporator.

Due to the complexity of the fluted tube geometry it is difficult to select the proper condenser size without the use of a computer program. The purpose of this paper is to describe the development of a simulation model for the design of fluted tube water heating condensers. The next section shows the philosophy followed to simulate both the water side and the refrigerant side of the fluted tube condenser. For the water side existing empirical equations found in the literature are used for both friction and heat transfer. However, on the refrigerant side no correlations are available in the literature to calculate friction and heat transfer coefficients. The approach thus followed in this paper is to use existing smooth tube correlations combined with enhancement ratios based on correlations available for helical coils and enhancement factors based on empirical data for fluted tube condensers.

2. Theoretical background

2.1. Fluted tube geometry

Fig. 1 shows a surface area view as well as a cross-sectional view of the fluted tube including the parameters describing the heat exchanger geometry. The outer diameter of the annulus is designated as D_o and is simply equal to the inside diameter of the outer tube.

Due to the complex flower-like shape of the inner fluted tube, the concept of “volume based diameters” is used rather than the conventional diameters associated with a circular cross-section. The volume based diameter is defined as the equivalent diameter of a circular cross-section that will result in the same enclosed volume inside the tube. The volume based

inside diameter of the fluted tube (D_{vi}) is therefore calculated as

$$D_{vi} = \sqrt{\frac{4Vol}{\pi L}} \tag{1}$$

with Vol the volume enclosed inside the fluted tube and L the length of the fluted tube. The volume based outside diameter of the fluted tube (D_{vo}) is calculated as

$$D_{vo} = D_{vi} + 2t \tag{2}$$

with t the wall thickness of the tube. The cross-sectional flow areas of the annulus and the fluted tube can therefore be calculated directly from D_o , D_{vo} and D_{vi} .

The other important geometric parameters are the flute depth (e) and the flute pitch (p) which are defined in Fig. 1. The flute depth and pitch are non-dimensionalised to obtain e^* and p^* respectively by dividing with D_{vi} . The helix angle (θ) is also required and is calculated as follows:

$$\theta = \arctan\left(\frac{\pi D_{vo}}{Np}\right) \tag{3}$$

with N the number of flute starts at any cross-section. The helix angle is also non-dimensionalised to θ^* by dividing by $\pi/2$.

2.2. Pressure drop

Three different pressure drop regions exists namely (i) single-phase pressure drop for the water flowing inside the inner fluted tube, (ii) two-phase refrigerant pressure drop in the annulus as well as (iii) single-phase refrigerant pressure drop for the superheated refrigerant gas and sub-cooled refrigerant liquid in the annulus.

2.2.1. Inner fluted tube

Arnold and Christensen et al. [1] have conducted extensive empirical work on flow inside fluted tubes and have developed correlations for the Darcy–Weisbach friction factor (see for instance Shames [2]). The friction factor (f) is dependent on the Reynolds number (Re_w) and geometry as follows: $Re_w < = 1500$

$$f = 0.554 \left(\frac{64.0}{Re_w - 45.0} \right) \times (e^*)^{0.384} (p^*)^{-1.454+2.083e^*} (\theta^*)^{-2.426} \tag{4}$$

$Re_w > 1500$

$$f = 1.209 (Re_w)^{-0.261} (e^*)^{1.26-0.05.p^*} (p^*)^{-1.66+2.033.e^*} (\theta^*)^{-2.699+3.67.e^*} \tag{5}$$

Re_w is based on the volumetric inside diameter (D_{vi}) and average water velocity.

2.2.2. Annulus

The annulus can effectively be simulated as a number of helical coils in parallel. A so-called ‘friction enhancement ratio’ is employed in both the single and two-phase regions to determine the pressure drop in the helical coils. The friction enhancement ratio (r_f) is defined as the ratio of the effective friction factors when comparing helical and straight tubes namely:

$$r_f = \frac{f_{\text{helical}}}{f_{\text{straight}}} \quad (6)$$

For the calculation of the friction enhancement ratio, f_{straight} is based on the standard single-phase correlation by Swamee and Jain [3] for straight tubes while f_{helical} is calculated from the single-phase correlation put forward by Das [4] for helical coils namely:

$$f_{\text{helical}} = 4 \left[0.079 \text{Re}_v^{-0.25} + 0.075 \left(\frac{D_{\text{ho}}}{d_{\text{coil}}} \right)^{0.5} + 17.5782 \text{Re}_v^{-0.3137} \left(\frac{D_{\text{ho}}}{d_{\text{coil}}} \right)^{0.3621} \left(\frac{e}{D_{\text{ho}}} \right)^{0.6885} \right] \quad (7)$$

In the correlation above D_{ho} is given by the difference between the inside diameter of the outer tube and the outside volumetric diameter (D_{vo}). d_{coil} is given by $D_{\text{ho}}/\sin\theta$. This single-phase enhancement ratio is assumed to also apply to the two-phase region. Therefore, once it has been determined, the pressure drop in the helical coils ($\Delta p_{\text{helical}}$) for both the single and two-phase regions can be calculated by obtaining the pressure drop in straight tubes ($\Delta p_{\text{straight}}$) and then multiplying it by r_f .

The two-phase pressure drop for straight tubes is dependent on the refrigerant quality and is based on the correlation by Traviss et al. [5] which states that:

$$\Delta p_{\text{straight}} = 0.09 \text{Re}_v^{-0.2} x^{1.8} \left[1 + 2.85 \left(\mu_x^{-0.1} \left(\frac{1-x}{x} \right)^{0.9} \rho_x^{0.5} \right)^{0.523} \right]^2 \frac{G^2}{\rho_v D_{\text{ho}}} \quad (8)$$

with G the mass flux. The refrigerant properties i.e. quality (x), density (ρ), and viscosity (μ) are determined at the average refrigerant temperature in the tube section being analysed. Re_v is based on the vapour properties of the refrigerant at the average temperature.

In the simulation model allowance was made for an additional enhancement factor (e_f) to account for the differences between standard helical coils and the actual fluted tube annulus. The total pressure drop was therefore calculated as:

$$\Delta p = e_f r_f \Delta p_{\text{straight}} \quad (9)$$

The value of the e_f was determined by comparing simulated results with measured data for a commercial fluted tube heat exchanger and will be addressed later on in the paper.

2.3. Heat transfer coefficients

Three different heat transfer modes are applicable namely (i) single-phase heat transfer for the water flowing inside the fluted tube, (ii) single-phase heat transfer for the superheated refrigerant gas and sub-cooled refrigerant liquid in the annulus as well as (iii) two-phase condensing heat and mass transfer in the annulus.

2.3.1. Inner fluted tube

The inside heat transfer coefficient is based on correlations from extensive empirical work by Arnold and Christensen et al. [1]. The Nusselt number (Nu) is dependent on the Reynolds number (Re_w) as follows: $\text{Re}_w < 5000$

$$\text{Nu} = 0.014 \text{Re}_w^{0.842} (e^*)^{-0.067} (p^*)^{-0.293} (\theta^*)^{-0.705} \text{Pr}^{0.4} \quad (10)$$

$\text{Re}_w > 5000$

$$\text{Nu} = 0.064 \text{Re}_w^{0.773} (e^*)^{-0.242} (p^*)^{-0.108} (\theta^*)^{0.599} \text{Pr}^{0.4} \quad (11)$$

The Prandtl number (Pr) is determined by $\text{Pr} = \frac{c_p \mu}{k}$ and the inside heat transfer coefficient by

$$h_i = \frac{\text{Nu}k}{D_{\text{vi}}}$$

2.3.2. Annulus

According to the Chilton–Colburn analogy (see for instance Incropera and DeWitt [6]) the heat transfer enhancement ratio (r_h) for simple geometries should be approximately equal to the friction enhancement ratio. Therefore, the Nusselt number for helical coils is calculated as:

$$\text{Nu}_{\text{helical}} = e_h r_h \text{Nu}_{\text{straight}} \quad \text{with } r_h = r_f \quad (12)$$

Allowance is again made for an additional enhancement factor (e_h) to cater for differences in the helical coil and fluted tube annulus as well as other deviations from the assumptions originally made in the friction-heat transfer analogy. The value of e_h was determined by comparison between the simulated and measured results and will be addressed later. It was again assumed that the single-phase enhancement ratios also apply to the two-phase region.

The calculation of $\text{Nu}_{\text{straight}}$ for the single-phase regions is based on the standard Dittus–Boelter correlation (Incropera and DeWitt [6]) namely:

$$\text{Nu}_{\text{straight}} = 0.023 \text{Re}^{0.8} \text{Pr}^{0.4} \quad (13)$$

The two-phase heat transfer coefficient is based on the technique used by Shah [7] where the liquid heat transfer coefficient (h_{liq}) is first determined with the aid of the Dittus–Boelter equation. This is then adjusted for the average quality of the refrigerant in the tube section being analysed as follows:

$$h_{tp} = h_{liq} \left[(1 - x)^{0.8} + \frac{3.8x^{0.76}(1 - x)^{0.04}}{pr^{0.38}} \right] \quad (14)$$

with pr equal to the ratio of the local static pressure to the critical pressure of the refrigerant.

3. Simulation model

The inputs to the condenser model are the fluted tube geometry, the refrigerant type, the refrigerant mass flow rate, the refrigerant inlet enthalpy where it leaves the compressor, as well as the water mass flow rate and inlet water temperature. The refrigerant inventory is not simulated based on a detailed void fraction model such as the one found in Orth [8]. The approach used is to fix the fraction of condenser volume that is filled with sub-cooled liquid refrigerant. The rationale for this is that due to the high density of the liquid, the volume of sub-cooled liquid in the system will remain virtually unchanged over a wide range of operating conditions. Our measurements have proven this to be a sufficiently accurate approach, especially given the deficiencies of current void fraction models. For this approach, either the degree of sub-cooling or the fraction of the volume containing sub-cooled liquid must therefore also be specified as input. The simulation model makes use of refrigerant property tables that can also be extended for zeotropic mixtures.

The simulation model is based on the algorithm shown in Fig. 3. Initial estimations are made for the size of the heat exchanger sections associated with the superheated and sub-cooled regions as well as the condensing temperature (T_{r2}). The heat exchanger area is divided up into a specified number of finite increments each representing a section of tubing as shown in the left of Fig. 4. This allows for the extension of the model to simulate heat exchangers for cycles employing zeotropic refrigerant mixtures. The number of areas is adjusted so that the phase interfaces coincide exactly with section interfaces. This means that the user specified number of areas is adjusted to include two extra areas as illustrated with the help of a pressure–enthalpy diagram in Fig. 4.

Given the geometry of each section, the heat transfer coefficients and pressure drops can now be determined using the correlations and enhancement factors described above. Once the pressure levels at each section interface are known, the inlet temperature, phase inter-

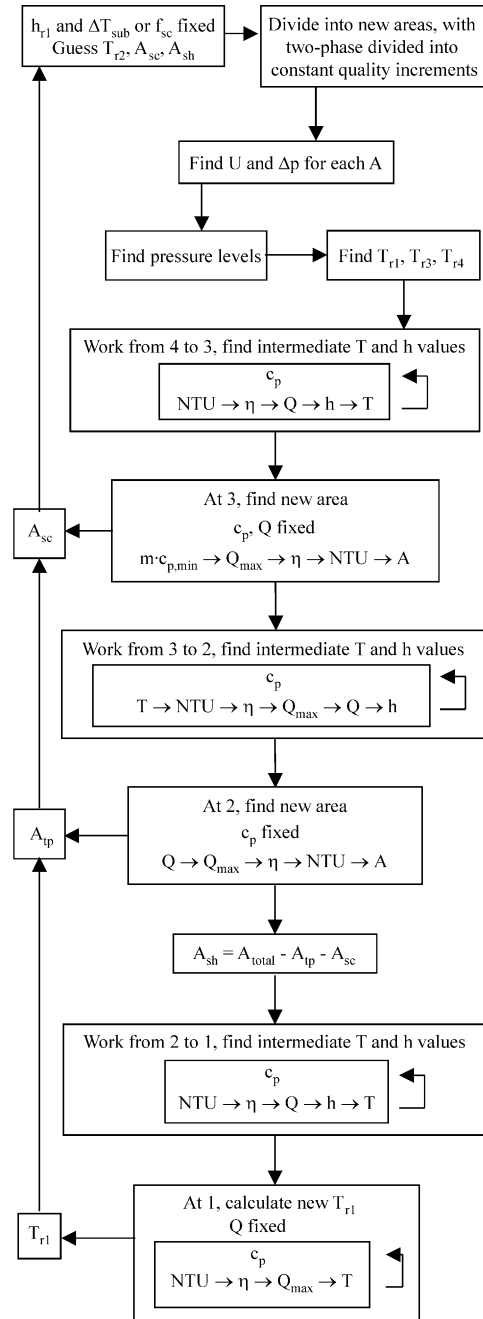


Fig. 3. Flow diagram for the condenser simulation routine.

face temperatures and outlet temperature can be obtained. Starting at the sub-cooled liquid side, each section is then solved iteratively to obtain a heat balance between the water and the refrigerant while the area of the section is adjusted to satisfy the effectiveness–NTU equation for counter-flow given the calculated heat transfer coefficient. Having worked through the whole condenser once, new superheat and sub-cooled areas as

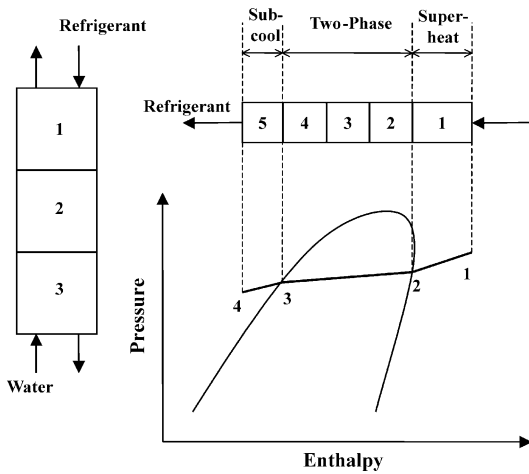


Fig. 4. Pressure-enthalpy diagram for the fluted tube condenser.

well as a new value for the condensing temperature are obtained. This whole procedure is then repeated until no further adjustments in areas or condensing temperature are required.

4. Verification

In order to obtain suitable values for the enhancement factors and to verify the simulation model, simulations were conducted for two commercial fluted tube heat exchangers for which results of independent tests were made available by the manufacturer. For each heat exchanger twelve sets of experimental data exists including for the refrigerant side: (i) condenser inlet pressure and temperature, (ii) condensation temperature, (iii) condenser outlet pressure and temperature, (iv) degree of sub-cool, and (v) mass flow rate. The experimental data for the waterside consisted of (i) inlet water pressure and temperature, (ii) outlet water pressure and temperature, and (iii) mass flow rate. The geometrical parameters of both fluted tube heat exchangers are listed in Table 1.

An optimisation routine was linked to the simulation model and used to obtain a single value for e_f and e_h resulting in the best fit between the empirical and simulated pressure drops and log mean temperature difference for all the data sets. The resultant values of e_f and e_h were 4.409 and 0.867 respectively.

Figs. 5–7 show the good comparison obtained between the simulated and measured results. The average difference between the simulated and measured pressure drops is 7.27% and the maximum difference is 30.76%. From the figures it can be seen that only one point, which corresponds to the same data set for all three graphs, shows a large error between the measured

Table 1
Geometrical parameters for two fluted tube heat exchangers

	Fluted coil 1	Fluted coil 2
Fluted tube material	Copper	Copper
Fluted length	6.9 m	8.0 m
Inside diameter of outside tube	40.8 mm	40.6 mm
Volume inside fluted tube	$3.93 \times 10^{-3} \text{ m}^3$	$3.66 \times 10^{-3} \text{ m}^3$
Number of flute starts	5	4
Flute depth	6.7 mm	6.8 mm
Flute pitch	12.1 mm	17.8 mm
Wall thickness of fluted tube	1.02 mm	0.97 mm

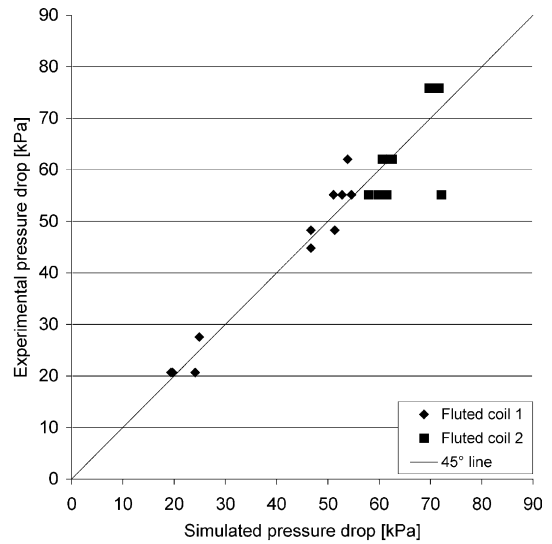


Fig. 5. Simulated versus measured pressure drop.

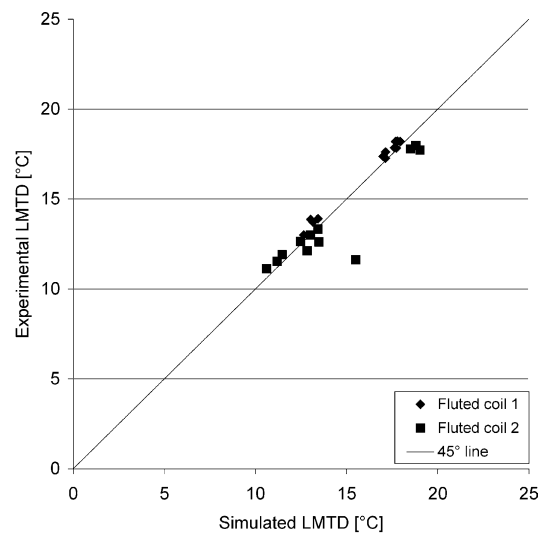


Fig. 6. Simulated versus measured log mean temperature difference.

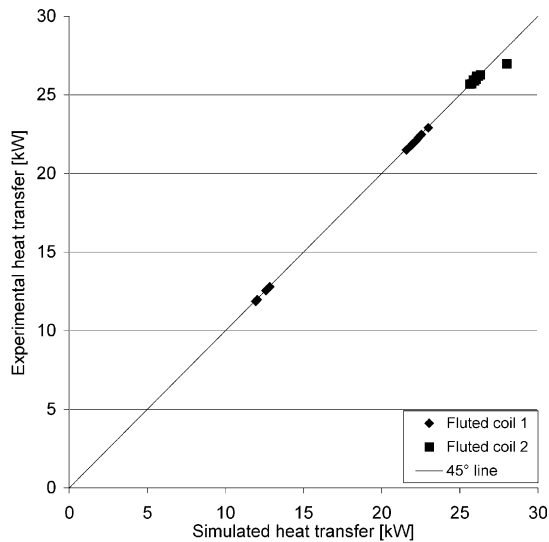


Fig. 7. Simulated versus measured heat transfer rate.

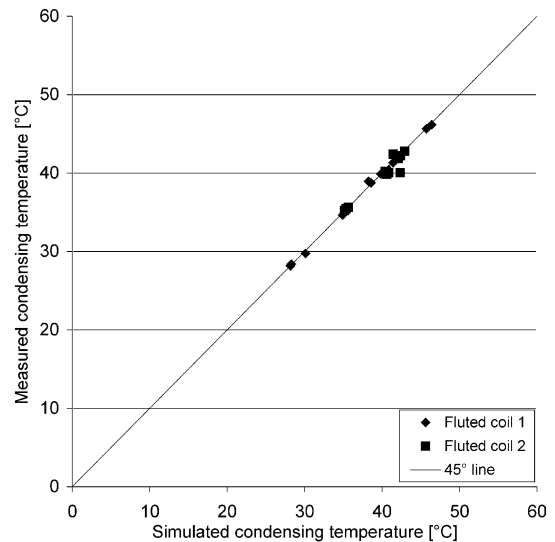


Fig. 8. Simulated versus measured condensation temperature.

and simulated results. Based on the accuracy obtained with all the other data points, it is suspected that this deviation may be due to inaccuracies in the measured data. If this single data point is ignored the average difference is 6.24% and the maximum difference 16.7%.

When comparing the log mean temperature difference (LMTD) between the simulated and measured results it can be seen from Fig. 6 that the average difference is 4.41% and the maximum difference is 33.25%. If the single deviating point is again ignored it results in an average difference of 3.19% and a maximum difference of 7.35%. Fig. 7 shows that the measurements covered a sufficiently wide range of heat transfer rates. The average difference between the simulated and measured heat transfer rates is 0.45% and the maximum difference is 3.81%. If the same data point as above is ignored the average difference is 0.3% and the maximum difference 0.65%.

Another important result is the condensation temperature obtained with the simulation model. The condensation temperature provides an indication of the head pressure provided by the compressor. In order to obtain the correct simulated refrigerant mass flow rate in the cycle, the simulated head pressure must be accurate. As shown in Fig. 8 the average difference between the simulated and measured condensation temperature is 0.91% and the maximum difference is 5.69%. If the same data point as above is ignored the average difference is 0.7% and the maximum difference 2.33%.

The value of $e_h = 0.867$ implies that if the heat transfer coefficient for simple helical coils were used on its own, the heat transfer rate would be over-predicted for the fluted tube annulus. This is mainly due to the fact that part of the heat transfer area of the annulus on the

outside of the outer tube is not in contact with the water inside the inner tube as can be seen from the fluted tube geometry in Fig. 1. This means that the effective heat transfer area in the fluted tube is approximately 87% of that of the analogous helical tube.

The value of $e_f = 4.409$ implies that the pressure drop in the fluted tube annulus is much higher than that of a corresponding smooth helical tube. This is realistic since the manufacturing process is such that the annulus is no longer simply a smooth channel but rather contains many indentations and rougher areas along the flow path.

Fig. 9 shows one example of the good comparison obtained for the temperature distribution through the

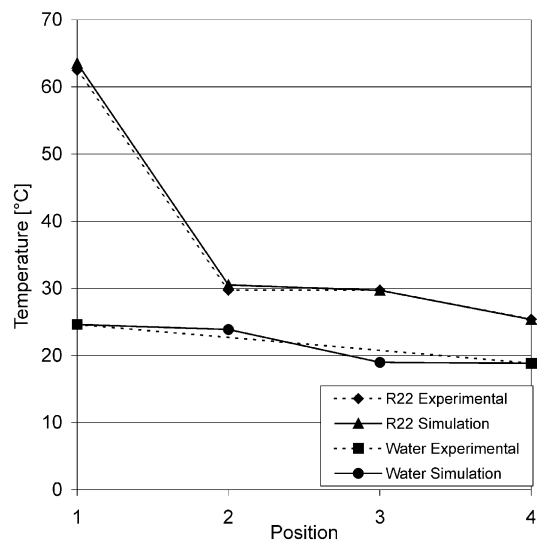


Fig. 9. Temperature distribution through condenser.

condenser on both the refrigerant and waterside. The reason for the straight line of the measured water temperature is that only the inlet and outlet water temperatures were obtained from the manufacturers, whereas the simulation determines the water temperature at each section of the condenser.

Even though the measurements of only two different fluted tubes were evaluated here, the results show that the approach followed here is valid. However, an extension of the study including results for a wider range of fluted tube heat exchangers would be desirable.

5. Conclusions

This paper described a detailed model to simulate fluted tube refrigerant-to-water condensers. The model allows the surface area to be divided into any number of sections for which all the refrigerant and water properties can be evaluated. This allows for the extension of the model to simulate heat exchangers for cycles employing zeotropic refrigerant mixtures. The model incorporates a simplified approach to simulate the influence of refrigerant charge that negates the need for a complicated void fraction model. The model is based on the effectiveness–NTU method and incorporates appropriate refrigerant-side heat transfer coefficients for the superheated, two-phase and sub-cooled regions given the detailed geometry of the heat exchanger. Existing empirical equations are used for both friction and heat transfer on the water side. However, on the refrigerant side no correlations are available in the literature to calculate friction and heat transfer coefficients. The use of existing smooth tube correlations

combined with enhancement ratios based on correlations available for helical coils as well as enhancement factors based on empirical data for fluted tube condensers are the approach used in this paper. The model was validated successfully with the aid of results from independent tests on two commercial fluted tube heat exchangers. The average difference between the simulated and measured pressure drops is 7.27% and the average difference for the log mean temperature difference (LMTD) is 4.41%. A need was however identified for an extension of the study to include results for a wider range of fluted tube heat exchangers.

References

- [1] Arnold JA, Garimella S, Christensen RN. Fluted tube heat exchanger design manual; 1993.
- [2] Shames IH. Mechanics of fluids. 3rd ed. Singapore: McGraw-Hill; 1992.
- [3] Swamee PK, Jain AK. Explicit equations for pipe-flow problems. *J Hydraulic Div Proc ASCE* 1976;657–64.
- [4] Das SK. Water flow through helical coils in turbulent condition. *The Canadian Journal of Chemical Engineering* 1993;71:971–3.
- [5] Traviss DP, Rohsenow WM, Baron AB. Forced convection condensation inside tubes: a heat transfer equation for condenser design. *ASHRAE Journal* 1973;79(1).
- [6] Incropera FP, DeWitt DP. Fundamentals of heat and mass transfer. 4th ed. Canada: John Wiley & Sons; 1996.
- [7] Shah MM. A general correlation for heat transfer during film condensation inside pipes. *International Journal of Heat and Mass Transfer* 1979;22:547–56.
- [8] Orth LA, Zietlow DC, Pedersen CO. Predicting refrigerant inventory of R-134a in air-cooled condensers. *ASHRAE Transactions* 1995;101(1):1367–75.